

Ionic metal  $K_xC_{60}$ : Cohesion and energy bands

Susumu Saito and Atsushi Oshiyama

*Fundamental Research Laboratories, NEC Corporation, Miyukigaoka, Tsukuba 305, Japan*

(Received 17 June 1991)

Microscopic total-energy electronic-structure calculations for  $K_xC_{60}$  show that solid  $C_{60}$  weakly bonded via van der Waals forces is transformed upon potassium doping into a strongly condensed *ionic metal* in which both Madelung and kinetic energies contribute to its large cohesive energy and bulk modulus. We also find that K doping induces lattice contraction which results in nonrigid energy-band modification. The Fermi level for  $K_3C_{60}$  is found to be located close to a peak of the density of states.

Fullerene  $C_{60}$  is a soccer-ball-shaped cluster with carbon atoms located at each vertex.<sup>1</sup> The earlier conjecture<sup>2</sup> on the unique shape has been indeed confirmed by success<sup>3</sup> in producing macroscopic quantities of  $C_{60}$  from carbon soot and by subsequent photoabsorption,<sup>3,4</sup> nuclear magnetic resonance,<sup>5</sup> and x-ray diffraction measurements.<sup>3,6</sup> In particular, the finding<sup>3</sup> of a close-packed crystalline form of  $C_{60}$  has triggered a considerable expansion of research on its solid-state properties: Photoemission<sup>7</sup> and inverse photoemission<sup>8</sup> studies on solid  $C_{60}$  have shown its peculiar electron states, and local-density calculations<sup>9,10</sup> have revealed that the  $C_{60}$  clusters are condensed by van der Waals forces and that the solid  $C_{60}$  is a semiconductor with a direct gap at the Brillouin-zone boundary.<sup>10</sup> Moreover, the recent discovery of superconductivity for the alkali-metal-doped fullerenes,  $K_xC_{60}$  (the critical temperature  $T_c=18$  K)<sup>11</sup> and  $Rb_xC_{60}$  ( $T_c=28$  K),<sup>12,13</sup> has raised fundamental questions as to mechanisms of superconductivity in these fullerene solids ("fullerites").

In this paper, we report microscopic total-energy electronic-structure calculations for  $KC_{60}$ ,  $K_2C_{60}$ , and  $K_3C_{60}$  in which potassium atoms are situated at either or both of tetrahedral and octahedral interstitial sites of face-centered-cubic (fcc)  $C_{60}$ . We have found that K doping in fcc  $C_{60}$  occurs exothermically with electron transfer from the K atom to the  $C_{60}$  cluster and at the same time with hybridization between K 4s,  $C_{60}$   $\pi$ , and  $C_{60}$   $\sigma$  orbitals. The resulting  $K_xC_{60}$  is shown to be an *ionic metal* in which both the electrostatic and kinetic energies contribute significantly to its larger cohesive energy and bulk modulus than those of undoped solid  $C_{60}$ . This feature of the material results from the uniqueness of the  $C_{60}$  cluster, i.e., its high electronegativity and closed-shell electron states, showing another possibility of the fullerenes as atomlike units to construct new exotic materials. We have also found that the K doping is accompanied by sizable *lattice contraction* which induces significant modification of the energy bands of fcc  $C_{60}$ . The Fermi level for  $K_3C_{60}$  is found to be located close to a peak of the calculated density of states (DOS). Although there is no experimental evidence that the fcc

lattice<sup>6</sup> of  $C_{60}$  is preserved in  $K_xC_{60}$ ,<sup>14</sup> the present results essentially hold in other lattice structures and clarify remarkable features in the modification of cohesive and electronic properties of the solid  $C_{60}$  upon alkali-atom doping.

The calculations have been performed with the local-density approximation<sup>15</sup> (LDA) using norm-conserving hard pseudopotentials<sup>16</sup> and the Gaussian-orbitals basis set as reported in Ref. 10. In addition to the Gaussian orbitals at the C sites, three *s* and two *p* Gaussian orbitals, whose exponents are determined by fitting the numerical pseudoatomic orbitals of a K atom, are placed at each K site in the lattice. Technical details of our method have been published elsewhere.<sup>17</sup> The present first-principles calculation describes accurately the structural properties (lattice constants, bulk moduli, and cohesive energies) of diamond and graphite.<sup>10</sup> The predicted cohesive energy of fcc  $C_{60}$  has been corroborated by recent experiment,<sup>18</sup> and the calculated DOS is in excellent agreement with the photoemission<sup>7,8</sup> and x-ray emission<sup>19</sup> data.

In fcc  $C_{60}$  lattice there are two tetrahedral and one octahedral interstitial sites per  $C_{60}$ .<sup>20</sup> The tetrahedral and octahedral sites have sufficient room to accommodate spheres of radius 1.1 and 2.1 Å, respectively. Since the ionic radius of  $K^+$  is about 1.3 Å, the two interstitial sites are candidates to accommodate K atoms. We thus place K atoms at one of these ( $KC_{60}$ ), at two tetrahedral ( $K_2C_{60}$ ), and at all of these ( $K_3C_{60}$ ) interstitial sites in fcc  $C_{60}$ , and minimize the total energy by varying the fcc lattice constant. In Fig. 1 the calculated total energies of  $KC_{60}$ ,  $K_2C_{60}$ , and  $K_3C_{60}$  as a function of the fcc lattice constant are shown. In the case of  $KC_{60}$  we find that the total energy with the K atom at the tetrahedral site is lower than that at the octahedral site by 1.8 eV per K atom. As is seen from the contour map of the valence electron density (Fig. 2), significant electron transfer to the  $C_{60}$  cluster from the K atom at any interstitial site occurs. The calculated cohesive energies for  $KC_{60}$ ,  $K_2C_{60}$ , and  $K_3C_{60}$  are 10.1 eV per  $KC_{60}$ , 19.3 eV per  $K_2C_{60}$ , and 24.2 eV per  $K_3C_{60}$ , respectively. The preference of the tetrahedral site (i.e., zinc-blende  $KC_{60}$ ) over the octahedral site (i.e., sodium

chloride  $KC_{60}$ ) is consistent with an argument based on a simple rigid-sphere model for the crystal structures of ionic materials.<sup>21</sup> Yet the Madelung energy for  $KC_{60}$  is estimated to be 3 eV (note the large distance between the K atom and the  $C_{60}$  cluster compared with the cation-anion distance in typical ionic materials.) Therefore the large cohesive energy obtained in the present calculation is explained not only by the Madelung energy but also by the kinetic-energy gain. The bulk modulus of  $KC_{60}$  obtained from the parabola fitting of the total energies is 77 GPa, and those of  $K_2C_{60}$  and  $K_3C_{60}$  are larger than that. Since the calculated cohesive energy and the bulk modulus of fcc  $C_{60}$  is 1.6 eV per  $C_{60}$  and 48 GPa,<sup>22</sup> respectively, the K doping transforms the fcc  $C_{60}$  weakly bonded via van der Waals force into a new strongly condensed ionic material. The reaction of K doping is indeed exothermic, and the calculated heats of formation for the reactions,  $C_{60}(\text{fcc})+K(\text{atom})\leftrightarrow KC_{60} + \Delta E_1$ ,  $KC_{60}+K(\text{atom})\leftrightarrow K_2C_{60} + \Delta E_2$ , and  $K_2C_{60}+K(\text{atom})\leftrightarrow K_3C_{60} + \Delta E_3$ , are  $\Delta E_1=8.5$  eV,  $\Delta E_2=9.2$  eV, and  $\Delta E_3=4.9$  eV, respectively. Further, phase separation of  $C_{60}(\text{fcc})$  and K metal is not likely since the cohesive energy of K metal is small compared with the above heats of formation.

We also find that the K doping is accompanied by siz-

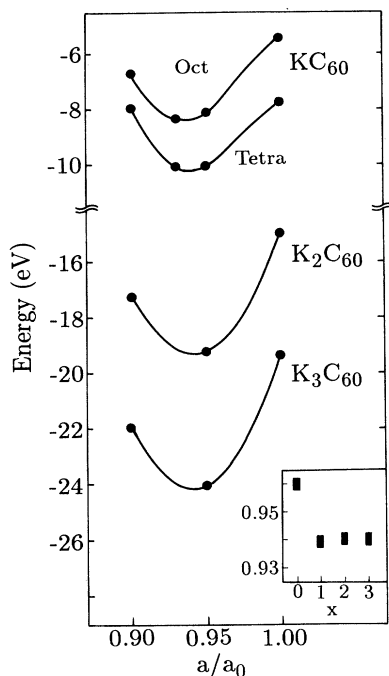


FIG. 1. Calculated total energies of  $K_xC_{60}$  as a function of the fcc lattice constant. The total energies are measured from the sum of the energies of isolated  $C_{60}$  cluster and of isolated  $x$  potassium atoms; i.e., the minus of the cohesive energies. The lattice constant is normalized to the experimental value of fcc  $C_{60}$  ( $a_0=14.198$  Å). The inset is the calculated lattice constant as a function of the K composition  $x$ .

able contraction of the fcc lattice constant: The calculated lattice constant for fcc  $C_{60}$  is 96% of the corresponding experimental value (14.198 Å),<sup>6</sup> whereas the values obtained for  $K_xC_{60}$  are about 94% (the inset of Fig. 1). This 2% difference corresponds to 0.3 Å. The LDA calculation gives highly accurate lattice constant (typically with less than 1% error) for condensed materials, whereas it underestimates the lattice constant of van der Waals solid such as graphite or fcc  $C_{60}$  by  $\sim 5\%$ .<sup>10</sup> Therefore the lattice contraction may be observed more prominently. In any case the obtained lattice contraction by the order of half an angstrom increases the electrostatic energy gain in  $K_xC_{60}$  on one hand, and modifies strongly the energy bands (shown below) causing the metallic energy gain in the material on the other. This contraction is in sharp contrast with the case of graphite intercalation compounds<sup>23</sup> (GIC) in which distance between adjacent graphite layers increases by  $\sim 50\%$  upon K intercalation. In first-stage GIC,  $KC_8$ , the nearest-neighbor distance between K atoms is 4.9 Å whereas in  $KC_{60}$  it is 5.7 Å

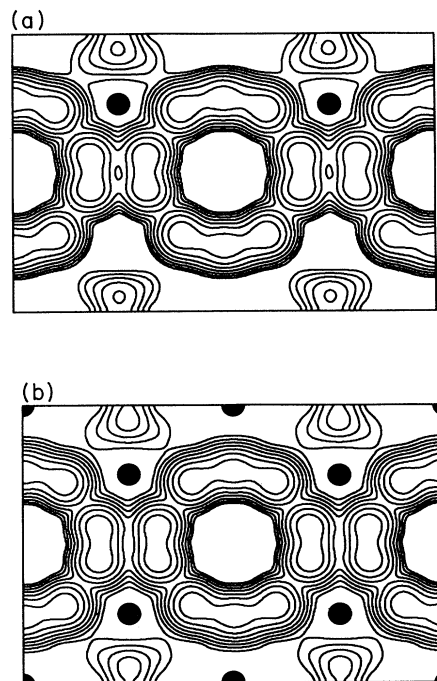


FIG. 2. Contour maps of the valence-electron densities of (a)  $KC_{60}$  and of (b)  $K_3C_{60}$  on the (110) plane. Solid circles denote the positions of the K atoms at (a) the tetrahedral, or at (b) the tetrahedral and the octahedral interstitial sites. The highest-density contour is 0.90 electron/Å<sup>3</sup>, and each contour represents twice or half the density of the adjacent contours. We observe the enhanced bonding between the  $C_{60}$  clusters due to the lattice contraction, and the electron transfer from the K atoms to the  $C_{60}$  clusters. The density (not shown here) at 2 Å apart from the octahedral site is about 0.002 electron/Å<sup>3</sup>.

which is also much larger than the corresponding value 4.6 Å in bcc K metal.

In Fig. 3 the calculated energy bands of  $K_3C_{60}$  are shown. The energy bands with  $\pi$  character become significantly dispersive compared to the bands of fcc  $C_{60}$ . This is a consequence of the lattice contraction and the resulting increased hybridization. The energy gap of fcc  $C_{60}$ , 1.5 eV, is reduced to 0.8 eV in  $K_3C_{60}$  according to the present LDA calculation. The Fermi level is at 1.25 eV above the valence-band top and is in the conduction bands. Analysis of the wave functions shows that the states at  $\sim 3$  eV above the Fermi level have appreciable character of both  $\pi$  orbitals and 4s orbitals at the tetrahedral site. On the other hand, a state at 3.9 eV above the Fermi level at the  $\Gamma$  point clearly holds the character of 4s at the octahedral site. The antibonding  $\sigma$  bands are also mixed with the  $\pi$  bands. It is noted that this nonrigid modification of the energy bands upon K doping occurs within the fcc structure and is not accompanied with structural phase transition. We also find that the band modification has already occurred for  $KC_{60}$  and that further K doping fills the electron in the conduction bands which still preserve the character of  $\pi$  orbitals of the fullerene.

It is clear from Fig. 3 that slight doping of K atoms forms an electron pocket around the  $X$  point. Yet the Fermi level for  $KC_{60}$  is already above the lowest conduction band at the  $W$  point so that its Fermi surface has holelike orbits around the  $\Gamma$  point near the (001) plane. Further, there are open orbits in the [001] direction.<sup>24</sup> This complexity of the Fermi surface results from the existence of two inequivalent  $XW$  lines causing unusual splitting and dispersion of the triply degenerate (at the  $\Gamma$  point) conduction bands. This inequivalence is characteristic of fullerenes; i.e., the internal atomic structure of the fullerene lowers the symmetry of the lattice system and affects the electron states. In the case of  $K_3C_{60}$ , the Fermi level is in the second conduction band so that

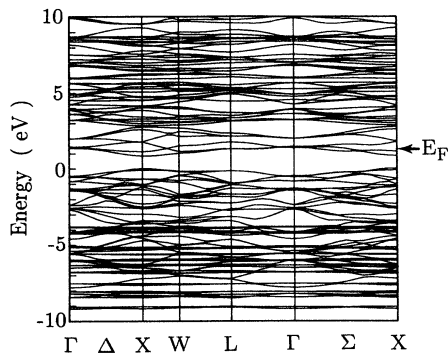


FIG. 3. Energy-band structure of  $K_3C_{60}$  along with the Fermi energy  $E_F$ . The valence-band top is defined as the zero energy. In addition to the  $XW$  line shown here, there is another inequivalent  $XW$  line on which the bands exhibit different dispersions.

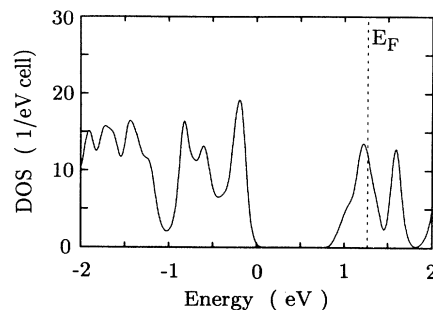


FIG. 4. The calculated electron density of states for  $K_3C_{60}$ . A cell contains one  $K_3C_{60}$ , and the valence-band top is defined as the zero energy. The Fermi level is close to the DOS peak. Note that the valence-band DOS is higher than the conduction-band DOS.

there occur other electron pockets around the  $X$  and the  $W$  points. Therefore  $K_3C_{60}$  is a metal characterized as a multicarrier system. The calculated DOS for  $K_3C_{60}$  is shown in Fig. 4. There are several DOS peaks originating from the nondispersive conduction bands along the symmetry  $k$  lines. The Fermi level for  $K_3C_{60}$  is found to be close to one of those DOS peaks. A recent experiment<sup>13</sup> has suggested that the composition of the superconducting phase of  $K_xC_{60}$  is close to  $x=3$ . The calculated Fermi-level density of states is  $N(E_F)=12$  states/(eV  $K_3C_{60}$ ). This rather high density of states would be a possible origin of the observed superconductivity in  $K_xC_{60}$ .<sup>25</sup>

The lattice contraction upon alkali-atom doping we have found is consistent with the observed variation in the superconducting critical temperature  $T_c$  with changing the dopant from K to Rb. The ionic radius of  $Rb^+$  (1.48 Å) is larger than that of  $K^+$  by 11%. The Rb atom at the tetrahedral site is thus unlikely to cause the lattice contraction as the K atom does. Therefore the energy bands become narrower and the  $N(E_F)$  higher so that the  $T_c$  increases. Another candidate for increasing  $N(E_F)$  is the halogen atoms which are expected to dope holes in the valence band of fcc  $C_{60}$ . The large ionic radius (1.95 Å for  $Br^-$  and 2.16 Å for  $I^-$ ) prevents the lattice contraction, but still fits in the octahedral site in the fcc lattice. Moreover, the peak of the valence-band DOS is higher than that in the conduction-band DOS (Fig. 4), reflecting the fact<sup>10</sup> that the valence-band effective masses,  $1.5m_e$  and  $3.4m_e$  ( $m_e$  is the bare electron mass), are heavier than the conduction-band effective mass  $1.3m_e$  in fcc  $C_{60}$ . This favors the higher  $N(E_F)$  in the case of halogen-atom doping. It is found that 1.6 states are available between the valence-band top and the first valence-band DOS peak in Fig. 4.

In conclusion, the present calculations have revealed that alkali-atom doping in fcc  $C_{60}$  transforms the unique semiconductor  $C_{60}$  into a novel form of solid, *ionic metal*  $K_xC_{60}$ . Potassium atoms induce the contraction of the fcc lattice constant, thus condensing the fullerenes. In addition, the Fermi level for  $K_3C_{60}$  is found to be close to the DOS peak, and the multiple Fermi surfaces exhibit complexity which reflects the internal structure of the

soccer-ball-shaped fullerene.

*Note added.* After the submission of the present paper, an x-ray diffraction measurement on  $K_3C_{60}$  has been reported [P. W. Stephens *et al.*, *Nature* **351**, 632 (1991)], and the orientation of  $C_{60}$  assumed in the present paper is found to be consistent with the experiment. The lattice constant reported there is, however, slightly larger than that of undoped solid  $C_{60}$ , in contradiction to the predic-

tion of the present work. The reason for this discrepancy is not clear yet.

We would like to thank Dr. Y. Miyamoto and Dr. N. Hamada for valuable discussion. We are also grateful to Professor J. H. Weaver and Professor J. L. Martins for providing their results prior to publication.

<sup>1</sup>For a review of early works, see H. W. Kroto, *Science* **242**, 1139 (1988).

<sup>2</sup>H. W. Kroto, J. R. Heath, S. C. O'Brien, R. F. Curl, and R. E. Smalley, *Nature (London)* **318**, 162 (1985).

<sup>3</sup>W. Krätschmer, L. D. Lamb, K. Fostiropoulos, and D. R. Huffman, *Nature (London)* **347**, 354 (1990).

<sup>4</sup>H. Ajie *et al.*, *J. Phys. Chem.* **94**, 8630 (1990).

<sup>5</sup>R. Taylor, J. P. Hare, A. K. Abdul-Sada, and H. W. Kroto, *J. Chem. Soc. Chem. Commun.* **20**, 1423 (1990); C. S. Yan-noni, R. D. Johnson, G. Meijer, D. S. Bethune, and J. R. Salem, *J. Phys. Chem.* **95**, 9 (1991).

<sup>6</sup>R. Fleming *et al.*, *MRS Late News Session on Buckeyballs: New Materials Made from Carbon Soot*, videotape (Materials Research Society, Pittsburgh, 1990).

<sup>7</sup>J. H. Weaver *et al.*, *Phys. Rev. Lett.* **66**, 1741 (1991).

<sup>8</sup>M. B. Jost *et al.*, *Phys. Rev. B* **44**, 1966 (1991).

<sup>9</sup>Q.-M. Zhang, J.-Y. Yi, and J. Bernholc, *Phys. Rev. Lett.* **66**, 2633 (1991).

<sup>10</sup>S. Saito and A. Oshiyama, *Phys. Rev. Lett.* **66**, 2637 (1991).

<sup>11</sup>A. Hebard *et al.*, *Nature (London)* **350**, 600 (1991).

<sup>12</sup>M. J. Rosseinsky *et al.*, *Phys. Rev. Lett.* **66**, 2830 (1991).

<sup>13</sup>K. Holczer *et al.*, *Science* **252**, 1154 (1991).

<sup>14</sup>The heavily doped samples regarded as  $Cs_6C_{60}$  and  $K_6C_{60}$ , which are presumably not the superconducting phases, are reported to be body-centered-cubic structure: O. Zhou *et al.*, *Nature (London)* **351**, 462 (1991).

<sup>15</sup>P. Hohenberg and W. Kohn, *Phys. Rev.* **136**, B864 (1964); W. Kohn and L. J. Sham, *ibid.* **140**, A1133 (1965).

<sup>16</sup>D. R. Hamann, M. Schlüter, and C. Chiang, *Phys. Rev. Lett.* **43**, 1494 (1979).

<sup>17</sup>Y. Miyamoto and A. Oshiyama, *Phys. Rev. B* **41**, 12 680 (1990); A. Oshiyama and M. Saito, *J. Phys. Soc. Jpn.* **56**, 2104 (1987).

<sup>18</sup>C. Pan, M. P. Sampson, Y. Chai, R. H. Hauge, and J. L. Margrave, *J. Phys. Chem.* **95**, 2944 (1991).

<sup>19</sup>Y. Saito *et al.*, *J. Phys. Soc. Jpn.* **60**, 2518 (1991).

<sup>20</sup>At each fcc lattice site a  $C_{60}$  cluster is oriented so that the point group becomes  $T_h$ . The bond lengths in the cluster are fixed to the experimental values, 1.46 and 1.40 Å. Actually, the "octahedral" interstitial site in the fcc lattice lacks the octahedral symmetry but has  $T_h$  symmetry because of the internal structures of the surrounding  $C_{60}$  clusters. Yet we use the term "octahedral" in this paper since it is practical.

<sup>21</sup>In general, ionic materials could have cesium chloride, sodium chloride, and zinc-blende structures. According to the rigid-sphere model, when the ionic radius of an anion is larger to some extent than that of a cation, the material is expected to have the zinc-blende structure. See, e.g., F. A. Cotton and G. Wilkinson, *Advanced Inorganic Chemistry* (Wiley, New York, 1972).

<sup>22</sup>In the recent experiments, the bulk modulus of fcc  $C_{60}$  is found to be smaller than the calculated value [S. J. Duclos *et al.*, *Nature (London)* **351**, 380 (1991); J. E. Fischer *et al.*, *Science* **252**, 1288 (1991)]. The fixed orientation and the fixed size of the  $C_{60}$  cluster may give larger bulk modulus in the present calculation.

<sup>23</sup>See, e.g., H. Kamimura, *Phys. Today* **40** (12), 64 (1987), and references therein.

<sup>24</sup>N. Hamada, S. Saito, Y. Miyamoto, and A. Oshiyama, *Jpn. J. Appl. Phys.* (to be published).

<sup>25</sup>See, for electron-phonon matrix elements, J. L. Martins, N. Troullier, and M. Schabel (unpublished). The details of their computational method are different from ours. (They use plane-wave basis set and soft pseudopotential.) Their band width and band gap of solid  $C_{60}$  are slightly different from our previous results (Ref. 10).